New high-pressure phases of $MoSe_2$ and $MoTe_2$

Oto Kohulák* and Roman Martoňák

Department of Experimental Physics, Faculty of Mathematics, Physics and Informatics, Comenius University in Bratislava, Mlynská dolina F2, 84248 Bratislava, Slovakia

(Received 22 November 2016; published 7 February 2017)

Three Mo-based transition-metal dichalcogenides MoS_2, $MoSe_2$, and $MoTe_2$ share at ambient conditions the same structure $2H_c$, consisting of layers where Mo atoms are surrounded by six chalcogen atoms in trigonal prism coordination. The knowledge of their high-pressure behavior is, however, limited, particularly in case of $MoSe_2$ and $MoTe_2$. The latter materials do not undergo a layer-sliding transition $2H_c \rightarrow 2H_a$ known in MoS_2 and currently no other stable phase aside from $2H_c$ is known in these systems at room temperature. Employing evolutionary crystal structure prediction in combination with *ab initio* calculations, we study the zero-temperature phase diagram of both materials up to Mbar pressures. We find a tetragonal phase with space group *P4/mmm*, previously predicted in MoS_2, to become stable in $MoSe_2$ at 118 GPa. In $MoTe_2$, we predict at 50 GPa a transition to a new layered tetragonal structure with space group *I4/mmm*, similar to CaC_2, where Mo atoms are surrounded by eight Te atoms. The phase is metallic already at the transition pressure and becomes a good metal beyond 1 Mbar. We discuss chemical trends in the family of Mo-based transition-metal dichalcogenides and suggest that $MoTe_2$ likely offers the easiest route towards the post-$2H$ phases.

DOI: 10.1103/PhysRevB.95.054105

I. INTRODUCTION

Transition-metal dichalcogenides (TMD) are mostly layered materials with composition MX_2, where M is transition metal such as W, Mo, Ti, Nb, Ta, etc., and X is a chalcogen such as S, Se, Te. While studied since long ago [1,2], they are currently of large interest, recently partly motivated also by the possibility of preparing graphenelike monolayers [3–6]. Their bulk phases exhibit a broad spectrum of electronic behavior, from insulator to semiconductor to superconductor [6]. Aside from that they exhibit also rich structural diversity, which is related to two possibilities for local sixfold coordination (trigonal prism or octahedral), number of layers in the unit cell, and stacking order, resulting in number of possible structures, such as $1T$, $2H$, $3R$, etc. [1]. It is well known that their electronic properties can be modified by doping [7]. Another important instrument allowing to tune their properties is pressure which can induce structural as well as electronic transitions.

In this study, we focus on Mo-based TMDs which include MoS_2, $MoSe_2$, and $MoTe_2$. At ambient conditions, all three compounds adopt a stable hexagonal $2H_c$ structure, where Mo atoms are in trigonal prism coordination [1]. This form is semiconducting with an indirect gap around 1 eV. Aside from this form, MoS_2 and $MoSe_2$ are also known in metastable $3R$ form which differs from $2H_c$ only by layer stacking. On the other hand, $MoTe_2$ can be prepared also in metallic metastable β-$MoTe_2$ monoclinic structure (space group $P2_1/m$) with distorted octahedral layers [8]. Unlike $2H_c$ (also called α-$MoTe_2$), this form is semimetallic at ambient pressure. Aside from the β-form also an orthorhombic T_d structure with distorted layers is known [9].

Among the three compounds, the most studied one under pressure is MoS_2. It has been studied experimentally up to 38.8 GPa in Ref. [10] where an unexplained structural transition was found around 20 GPa. The results of this study were theoretically explained in Ref. [11] by proposing a phase transition consisting of layer sliding. This interpretation was experimentally confirmed in Refs. [12,13] where the system was studied up to 51 and 81 GPa, respectively. In the latter study, MoS_2 was also found to undergo a metallization transition resulting from band overlap between 30–40 GPa, in agreement with theoretical prediction in Ref. [11]. The behavior at even higher pressure in the Mbar range was recently studied experimentally [14] and theoretically in Ref. [15]. While the theoretical work [15] predicted a phase transition to a new tetragonal phase with space group *P4/mmm* at 138 GPa or a chemical decomposition at 135 GPa to MoS and elemental sulfur, experimentally no structural transition was observed up to 200 GPa. The discrepancy can most likely be attributed to the slow kinetics at high-pressure conditions.

In Ref. [16], the possibility of a layer-sliding transition, similar to that in MoS_2, was studied theoretically in $MoSe_2$ and $MoTe_2$. It was shown that in these materials the $2H_a$ structure is actually less stable than the $2H_c$ one, due to larger volume, and therefore no sliding transition takes place. The systems were predicted to metallize at 40 and 19 GPa, respectively. This result for $MoSe_2$ was confirmed in Ref. [17] together with the lack of sliding transition up to 60 GPa. In Ref. [16], however, no structural search was performed in order to identify possible transitions to other structures in $MoSe_2$ and $MoTe_2$. Nothing is therefore known about the behavior of $MoSe_2$ beyond 60 GPa, either theoretically or experimentally. In case of $MoTe_2$, a lot of experimental activity was recently devoted to study of its properties at ambient pressure. Main interest was given to its orthorhombic phase T_d which was proposed [18] and more recently proven to be a type-II Weyl semimetal [19]. Possible transitions to other stable structures at high pressure, however, remain unknown.

In this paper, we aim at filling the gap in understanding of the high-pressure behavior of $MoSe_2$ and $MoTe_2$ up to Mbar pressures. By applying evolutionary algorithms [20] in combination with *ab initio* calculations we predict new phases and analyze their properties. The paper is organized as follows. In Sec. II we present the *ab initio* and evolutionary algorithms

*Corresponding author: kohulak@fmph.uniba.sk

approach we used. In Sec. III we present our predictions for structures of both materials and analyze their properties. In the final Sec. IV we discuss the results and draw conclusions.

II. METHODS

For our evolutionary search we have used the XTALOPT package [21] in combination with *ab initio* structural optimization implemented in QUANTUM ESPRESSO [22] and VASP [23] packages. We employed the projector augmented-wave (PAW) method [24,25] and the exchange-correlation energy was calculated with the PBE functional [26]. Similarly to Refs. [11,15,16], also here we decided not to apply van der Waals (vdW) corrections in structural relaxations at high pressure (including the evolutionary searches). In Ref. [16] (Fig. 2), we compared our theoretical predictions for the lattice parameter c in $2H_c$-$MoSe_2$ with the experimental data from Ref. [27]. It can be seen that at pressures beyond 15 GPa, the PBE calculation agrees very well with the experimental data, justifying our approach. For calculation with VASP we have used PAW pseudopotentials (PP) with 14, 6, and 6 valence electrons for Mo, Se, and Te, respectively. For calculation with QUANTUM ESPRESSO we have used PAW PP with the same number of valence electrons for Mo and Se but we used 16 valence electrons for Te.

For enthalpy calculations we have used the VASP package [23] where the energy cutoff was set to 400 eV. K-point grid for Monkhorst-Pack scheme [28] was generated with ASE package [29] with desired density of 7 points/Å^{-1}. Electronic band structure calculations were performed with QUANTUM ESPRESSO [22] package and the spin-orbit coupling was neglected. We have used cutoff 80 Ry and K-point grid $18 \times 18 \times 6$ for self-consistent calculation and $30 \times 30 \times 10$ for non-self-consistent calculation of the electron density of states. For phonon calculations we have used the QUANTUM ESPRESSO package [22] employing the density functional perturbation theory (DFPT). The energy cutoff for plane waves was chosen 70 Ry and the grid of q points was chosen $9 \times 9 \times 3$ in both materials.

We have performed various evolutionary searches with up to four formula units of $MoSe_2$ up to 150 GPa and up to eight formula units of $MoTe_2$ up to 110 GPa (for more details about search settings, see Supplemental Material [30]). For search in $MoSe_2$ we have used as a starting population only randomly generated structures. In case of $MoTe_2$ at 50 GPa we have also included some known structures such as hexagonal α-$MoTe_2$-$2H_c$, β-$MoTe_2$-$1T'$, and orthorhombic T_d while at 110 GPa we included $2H_c$ and the already known *I4/mmm* in order to speed up the calculations. The number of structures generated in all searches performed are shown in Table 1 in the Supplemental Material [30]. Our results are valid within the usual limitations of structural search, in particular the limited number of atoms in the simulation cell and the limited number of generated structures.

III. RESULTS

A. $MoSe_2$

In our structural search we found several known as well as new structures. The enthalpies of the relevant low-enthalpy ones as function of pressure are shown in Fig. 1. The ambient pressure layered phase $2H_c$ remains stable up to remarkably high pressure of 118 GPa. At 118 GPa, a tetragonal *P4/mmm* (No. 123) phase, analogous to that predicted in Ref. [15] for MoS_2, becomes more stable, accompanied by decrease of volume by 3.7%. At 120 GPa the lattice parameters are $a = 2.854$ Å and $c = 8.590$ Å, Mo atoms are on Wyckoff positions $2h$ (0.5, 0.5, 0.166) and Se atoms are on $1d$ (0.5, 0.5, 0.5), $2g$ (0.0, 0.0, 0.321), and $1a$ (0.0, 0.0, 0.0) positions. This new phase is a good metal as can be seen in Fig. 2, where the electronic band structure and the density of states are plotted.

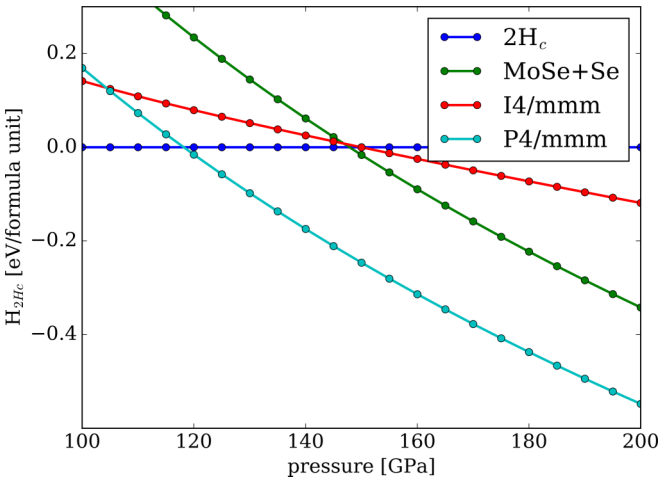

FIG. 1. Enthalpy as function of pressure for $MoSe_2$ structures (calculated with VASP). Enthalpies are relative to the $2H_c$ phase.

Assuming that direct transition to the *P4/mmm* phase might be difficult for kinetic reasons, as discussed in Ref. [15], it is justified to consider possible transitions to metastable phases that compete with $2H_c$ at pressures beyond 118 GPa. At 150 GPa, there are two phases that nearly simultaneously become more stable than $2H_c$. One of them represents chemical decomposition to MoSe + Se, where MoSe adopts

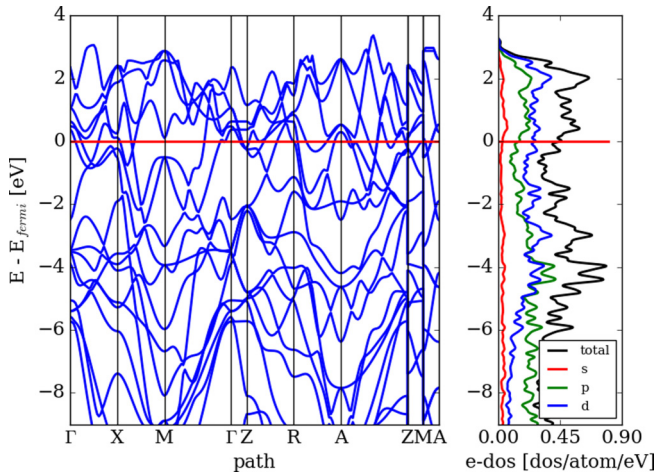

FIG. 2. Band structure and projected density of states of $MoSe_2$-*P4/mmm* phase at 118 GPa. Last two sections are paths between $X \rightarrow R$ and $M \rightarrow A$.

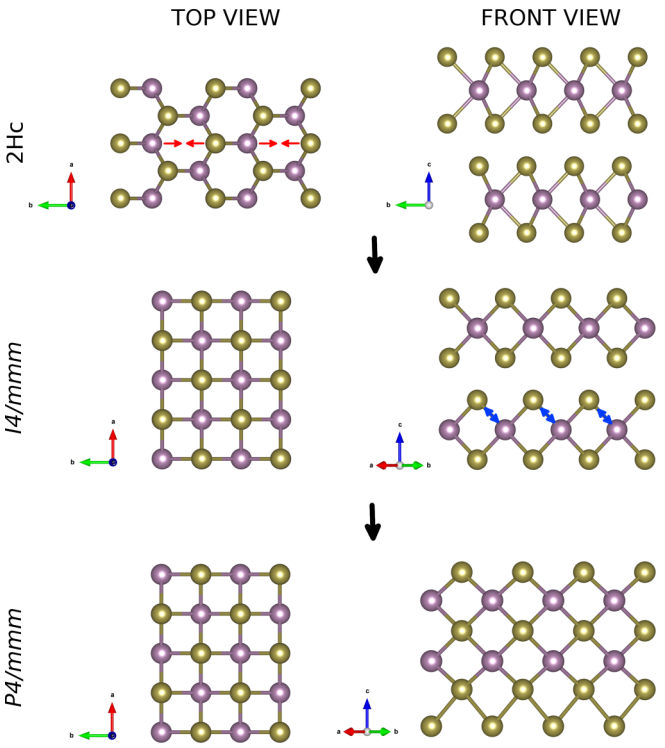

FIG. 3. Tentative phase transition mechanism between $2H_c$ (top panel) and *I4/mmm* structures (middle panel) could proceed via uniaxial compression as schematically indicated by red arrows. The other speculated phase transition between *I4/mmm* and *P4/mmm* structures (bottom panel) can occur by exchange of positions between Mo and chalcogen atoms (indicated by blue arrows). Structures were visualized by VESTA package [32].

the CsCl structure, again similarly to the case of MoS_2 [15] and Se the Se-VI structure [31]. Since the structure of MoSe at the conditions of the phase transition was unknown, an additional evolutionary search was performed and indeed confirmed the CsCl structure. For similar kinetic reasons as in case of *P4/mmm*, we believe that such decomposition might not be easily observed, at least at room temperature. A plausible scenario therefore appears to be a transition to a tetragonal phase with space group *I4/mmm* (No. 139) which becomes stable with respect to $2H_c$ at 150 GPa. This phase also represents a layered structure (Fig. 3), however, Mo atom now has an eightfold rather than sixfold coordination. While the structure is somewhat similar to CaC_2 (the same space group), the lattice parameters ratio $\frac{c}{a}$ is substantially higher in *I4/mmm*-$MoSe_2$ and, therefore, in contrast to CaC_2 the new phase has a layered character. To our knowledge, such structure has never been observed in transition-metal dichalcogenides. The phase transition is accompanied by a small volume drop of 1.0%. Structural parameters of the *I4/mmm* phase at 150 GPa (equilibrium condition with $2H_c$ phase) are $a = 2.685$ Å and $c = 9.454$ Å with Mo atom at Wyckoff position $2a$ (0.0, 0.0, 0.0) and Se atom at $4e$ (0.5, 0.5, 0.845). It appears plausible to assume that this structure could be created from $2H_c$ via a simple uniaxial compression or shear bringing two more chalcogen atoms in the vicinity of Mo atom as shown schematically in Fig. 3 (see also the

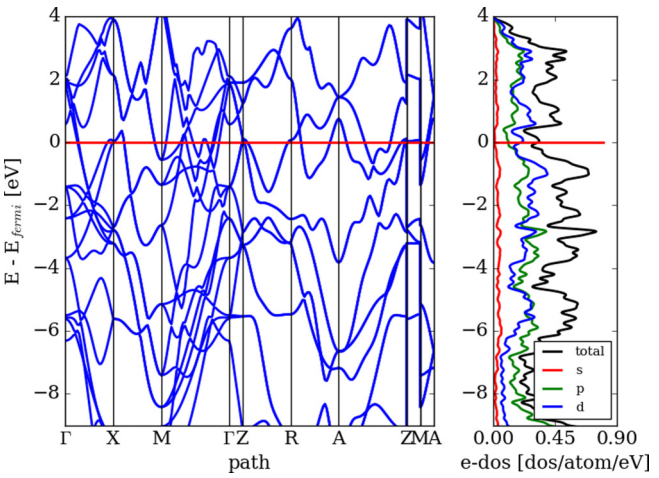

FIG. 4. Band structure and projected density of states of the $MoSe_2$-*I4/mmm* phase at 150 GPa. Last two sections are paths between $X \rightarrow R$ and $M \rightarrow A$.

Sec. III B). Since such mechanism does not require diffusion of atoms, the *I4/mmm* phase could possibly be more easily kinetically accessible compared to both *P4/mmm* phase and chemical decomposition. We thus predict it to be a likely candidate for the experimental outcome of compression of $2H_c$ beyond 150 GPa even though it is only metastable with respect to both *P4/mmm* and decomposition. We note that this structure was also found for MoS_2 in the study in Ref. [15], however, in that case it has enthalpy higher than $2H_a$ at 150 GPa by 0.51 eV per formula unit and therefore we did not consider it further.

In Fig. 4, we show the electronic band structure and density of states of the *I4/mmm* structure at 150 GPa. It is clear that the structure is metallic. The pressure evolution of the density of states at the Fermi level for this phase is shown in Fig. 5. It can be seen that the metallicity becomes stronger above 150 GPa as more bands cross the Fermi level. The most important

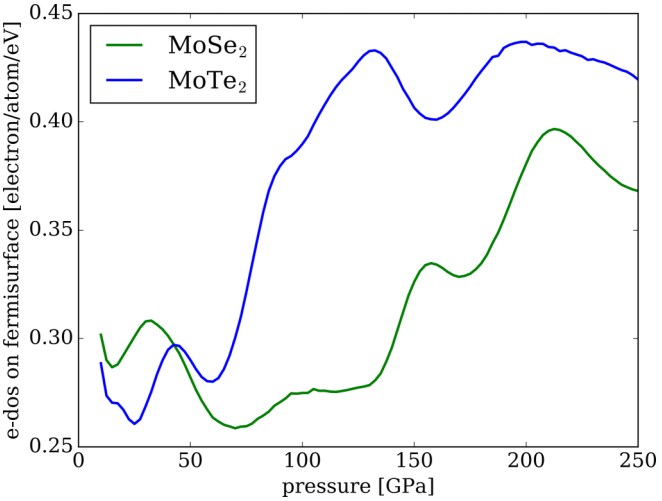

FIG. 5. Pressure evolution of the electronic density of states at the Fermi level of structure *I4/mmm*. In order to make the curves smoother, a Gaussian smearing with $\sigma = 0.06$ eV was performed.

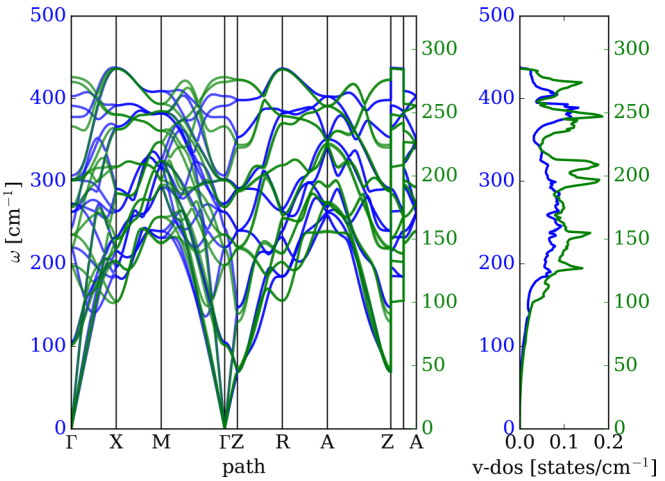

FIG. 6. Phonon dispersion curves of the *I4/mmm* structure. Blue and green lines are for $MoSe_2$ at 150 GPa and for $MoTe_2$ at 50 GPa, respectively. Last two sections are paths between $X \rightarrow R$ and $M \rightarrow A$.

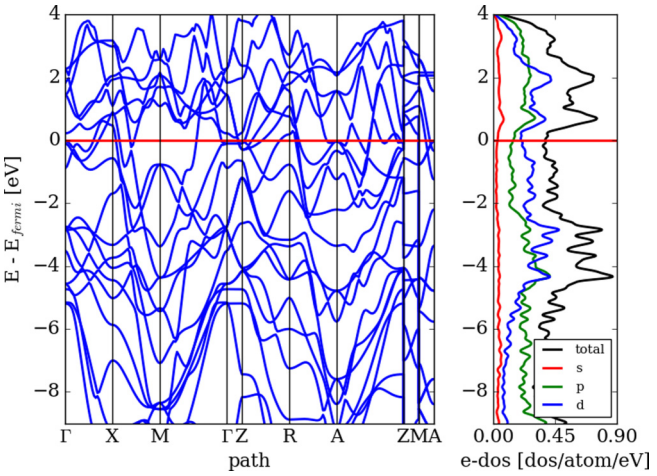

FIG. 8. Band structure and projected density of states of the $MoTe_2$-*P4/mmm* phase at 110 GPa. Last two sections are paths between $X \rightarrow R$ and $M \rightarrow A$.

contribution to states at the Fermi level originates from Mo-d states, in particular from the d_{xz} and d_{yz} states. Employing the QUANTUM ESPRESSO code we calculated in the *I4/mmm* phase at 150 GPa the electron-phonon coupling parameter and found a value of $\lambda \sim 0.42$. Applying the Allen-Dynes formula [33] and assuming $\mu^* = 0.1$, we predict a superconducting critical temperature of $T_c \approx 2$ K. Phonon dispersion curves are shown in Fig. 6.

B. $MoTe_2$

In $MoTe_2$, our structural search also found the same *P4/mmm* and *I4/mmm* structures as in the previous case. The enthalpies as function of pressure are shown in Fig. 7. In contrast to $MoSe_2$, however, here the transition to the *I4/mmm* at 50 GPa preempts the transition to *P4/mmm* as well as the instability with respect to chemical decomposition. We verified the possibility of the tentative $2H_c \rightarrow I4/mmm$ transition mechanism shown in Fig. 3 by simple simulation performing a gradual uniaxial compression of the $2H_c$ phase of $MoTe_2$ at $T = 0$. We found that such simulated compression indeed resulted in change of Mo atom coordination from six to eight and creation of the *I4/mmm* phase. The transition is accompanied by a volume drop of 1.8%. Upon further compression, the phase remains stable up to 110 GPa where the *P4/mmm* structure takes over. The lattice parameters of the *P4/mmm* phase at 110 GPa are $a = 3.041$ Å and $c = 9.471$ Å, Mo atoms are on Wyckoff positions $2g$ (0.0, 0.0, 0.340) and Te atoms are on $1d$ (0.5, 0.5, 0.5), $2h$ (0.5, 0.5, 0.189), and $1a$ (0.0, 0.0, 0.0) positions. Phase transition from *I4/mmm* to *P4/mmm* is accompanied by volume drop of 1.2%. Electronic band structure and density of states are plotted in Fig. 8, from which clear metallic character can be seen.

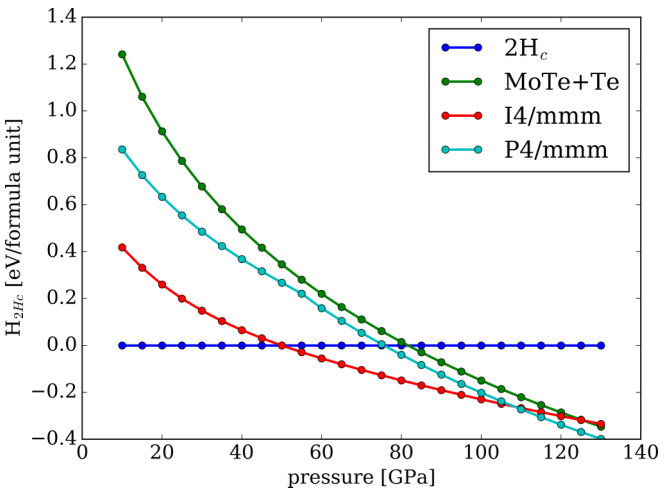

FIG. 7. Enthalpy as function of pressure for $MoTe_2$ structures (calculated with VASP). Enthalpies are relative to the $2H_c$ phase.

Since in case of $MoTe_2$ the *P4/mmm* phase appears after the *I4/mmm* where the eightfold coordination of Mo atoms already exists, it appears plausible that the kinetics of the transition $I4/mmm \rightarrow P4/mmm$ in $MoTe_2$ could be faster than that of direct transition $2H_c \rightarrow P4/mmm$ in $MoSe_2$ and MoS_2 which requires an increase of coordination of Mo atoms. A speculative simple mechanism for the $I4/mmm \rightarrow P4/mmm$ transition, consisting of exchange of positions between Mo and chalcogen atoms, is shown in Fig. 3. In this respect, we can speculate that the observed metastability of the $2H_a$ phase up to 200 GPa in Ref. [14] could be possibly related to the high enthalpy of the *I4/mmm* phase in MoS_2 which prevents it from acting as intermediate phase in creation of the *P4/mmm* phase.

Assuming MoTe adopts the same CsCl structure as found in case of MoS_2 and $MoSe_2$ and Te adopts the bcc Te-V [34] structure,[1] $MoTe_2$ does not appear to be prone to chemical decomposition at any pressure between 0 and 130 GPa.

Lattice parameters of the *I4/mmm* structure at 50 GPa (equilibrium condition with $2H_c$ structure) are $a = 3.036$ Å and $c = 11.095$ Å with Mo atom on Wyckoff position $2a$

[1]This structure was found at pressure of 27 GPa in Ref. [34] and we are not aware of experiments at higher pressure.

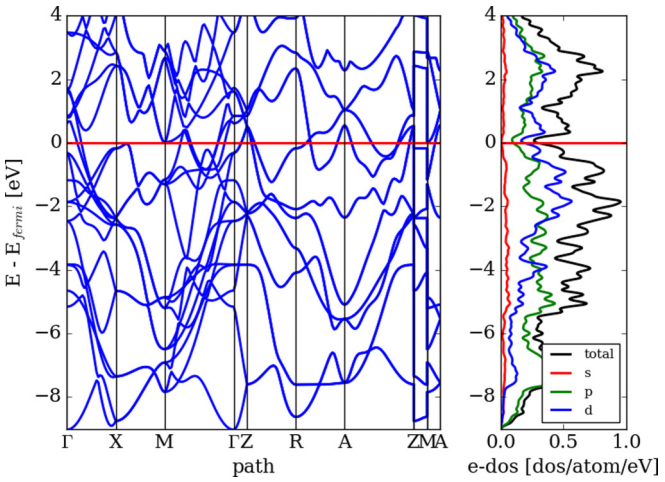

FIG. 9. Band structure and projected density of states of the $MoTe_2$-*I4/mmm* phase at 50 GPa. Last two sections are paths between $X \rightarrow R$ and $M \rightarrow A$.

(0.0, 0.0, 0.0), and Te atom on 4*e* (0.5, 0.5, 0.145). The band structure and electronic density of states are shown in Fig. 9. Projections of density of states show that the electronic states at the Fermi level are composed mostly of Mo-*d* orbitals (again mainly the d_{xz} and d_{yz} ones, see Fig. 1 in the Supplemental Material [30]). While the *I4/mmm* structure is metallic already at the transition pressure of 50 GPa, its metallicity substantially increases beyond 1 Mbar (see Fig. 5). Using the same procedure as in case of $MoSe_2$, we predict at 50 GPa a coupling parameter $\lambda = 0.46$ resulting in superconducting critical temperature of $T_c \approx 2$ K. Phonon dispersion curves are shown in Fig. 6.

Since the *I4/mmm* structure becomes stable at relatively low pressure of 50 GPa, it is natural to ask whether it could be quenched to ambient pressure. In order to test this hypothesis, we performed a short NPT MD run at $T = 300$ K and $p = 0$ GPa in a supercell consisting of 144 atoms. In this case, we also added the vdW correction employing the Grimme DFT-D2 method [35]. We observed after 4 ps a spontaneous transition to $2H$ structure with random stacking of layers, proceeding via mechanism essentially inverse to that described above for the $2H_c \rightarrow I4/mmm$ transition (Fig. 3). This shows that the *I4/mmm* phase of $MoTe_2$ cannot be quenched to ambient pressure.

IV. DISCUSSION AND CONCLUSIONS

Referring also to results found in Ref. [15] for MoS_2, we found three possible high-pressure structures to which the $2H$ MoX_2 compounds ($2H_c$ $MoSe_2$ or $MoTe_2$ and $2H_a$ MoS_2) can transform, namely, *P4/mmm*, *I4/mmm*, and chemical decomposition. Comparing the three compounds, clear chemical trends can be seen for the post-$2H$ phases. In case of MoS_2 chemical decomposition represents thermodynamically stable route since both *P4/mmm* and *I4/mmm* have higher and much higher enthalpy, respectively, and are only metastable. Decomposition could thus be possibly avoided only due to kinetic barriers. Moving towards heavier chalcogens from S to Se to Te, the picture changes. For $MoSe_2$ and $MoTe_2$, chemical decomposition does not become thermodynamically stable in the whole pressure range in which we have studied them. Instead, *P4/mmm* and in particular *I4/mmm* become more favorable and eventually thermodynamically stable, resulting in transition $2H_c \rightarrow P4/mmm$ in $MoSe_2$ at 118 GPa and $2H_c \rightarrow I4/mmm$ in $MoTe_2$ at 50 GPa. Since the *P4/mmm* phase becomes stable in $MoTe_2$ at 110 GPa, following $I4/mmm$, it appears likely that $MoTe_2$ might offer the easiest route to reach both post-$2H$ phases in Mo-based TMD. We suggest that our predictions for new metallic high-pressure phases in $MoSe_2$ and $MoTe_2$ be tested experimentally. Aside from pressure, it might be necessary to work at elevated temperatures in order to overcome the presumably slow kinetics. The high-pressure layered structure *I4/mmm* in both studied systems could possibly be interesting also as high-pressure lubricant, similarly to the case of MoS_2 at ambient pressure [36].

ACKNOWLEDGMENTS

This work was supported by the Slovak Research and Development Agency under Contract No. APVV-15-0496, by the VEGA Project No. 1/0904/15, and by the Project Implementation No. 26220220004 within the Research & Development Operational Programme funded by the ERDF. Part of the calculations were performed in the Computing Centre of the Slovak Academy of Sciences using the supercomputing infrastructure acquired in Projects ITMS No. 26230120002 and No. 26210120002 (Slovak infrastructure for high-performance computing) supported by the Research & Development Operational Programme funded by the ERDF.

[1] J. Wilson and A. Yoffe, Adv. Phys. **18**, 193 (1969).
[2] L. Gmelin, *Gmelin Handbook of Inorganic and Organometallic Chemistry*, Vol. B 7-9 (Springer, Berlin, 1995), p. 16.
[3] K. F. Mak, C. Lee, J. Hone, J. Shan, and T. F. Heinz, Phys. Rev. Lett. **105**, 136805 (2010).
[4] K. Chang and W. Chen, ACS Nano **5**, 4720 (2011).
[5] B. Radisavljevic, A. Radenovic, J. Brivio, V. Giacometti, and A. Kis, Nat. Nanotechnol. **6**, 147 (2011).
[6] Q. H. Wang, K. Kalantar-Zadeh, A. Kis, J. N. Coleman, and M. S. Strano, Nat. Nanotechnol. **7**, 699 (2012).
[7] R. B. Somoano, V. Hadek, and A. Rembaum, J. Chem. Phys. **58**, 697 (1973).
[8] B. E. Brown, Acta Crystallogr. **20**, 268 (1966).
[9] R. Clarke, E. Marseglia, and H. P. Hughes, Philos. Mag. B **38**, 121 (1978).
[10] R. Aksoy, Y. Ma, E. Selvi, M. C. Chyu, A. Ertas, and A. White, J. Phys. Chem. Solids **67**, 1914 (2006).
[11] L. Hromadová, R. Martoňák, and E. Tosatti, Phys. Rev. B **87**, 144105 (2013).
[12] N. Bandaru, R. S. Kumar, D. Sneed, O. Tschauner, J. Baker, D. Antonio, S.-N. Luo, T. Hartmann, Y. Zhao, and R. Venkat, J. Phys. Chem. C **118**, 3230 (2014).
[13] Z.-H. Chi, X.-M. Zhao, H. Zhang, A. F. Goncharov, S. S. Lobanov, T. Kagayama, M. Sakata, and X.-J. Chen, Phys. Rev. Lett. **113**, 036802 (2014).
[14] Z. Chi *et al.*, arXiv:1503.05331.

[15] O. Kohulák, R. Martoňák, and E. Tosatti, Phys. Rev. B **91**, 144113 (2015).
[16] M. Rifliková, R. Martoňák, and E. Tosatti, Phys. Rev. B **90**, 035108 (2014).
[17] Z. Zhao, H. Zhang, H. Yuan, S. Wang *et al.*, Nat. Commun. **6**, 7312 (2015).
[18] A. A. Soluyanov, D. Gresch, Z. Wang, Q. Wu, M. Troyer, X. Dai, and B. A. Bernevig, Nature (London) **527**, 495 (2015).
[19] Y. Qi *et al.*, Nat. Commun. **7**, 11038 (2016).
[20] A. Oganov and C. Glass, J. Chem. Phys. **124**, 244704 (2006).
[21] D. C. Lonie and E. Zurek, Comput. Phys. Commun. **182**, 372 (2011).
[22] P. Giannozzi *et al.*, J. Phys.: Condens. Matter **21**, 395502 (2009).
[23] G. Kresse and J. Hafner, Phys. Rev. B **47**, 558 (1993).
[24] P. E. Blöchl, Phys. Rev. B **50**, 17953 (1994).
[25] G. Kresse and D. Joubert, Phys. Rev. B **59**, 1758 (1999).
[26] J. P. Perdew, K. Burke, and M. Ernzerhof, Phys. Rev. Lett. **77**, 3865 (1996).
[27] R. Aksoy, E. Selvi, and Y. Ma, J. Phys. Chem. Solids **69**, 2138 (2008).
[28] H. J. Monkhorst and J. D. Pack, Phys. Rev. B **13**, 5188 (1976).
[29] S. R. Bahn and K. W. Jacobsen, Comput. Sci. Eng. **4**, 56 (2002).
[30] See Supplemental Material at http://link.aps.org/supplemental/10.1103/PhysRevB.95.054105 for more information about evolutionary searches and projected electronic density of states.
[31] O. Degtyareva, E. Gregoryanz, M. Somayazulu, H.-k. Mao, and R. J. Hemley, Phys. Rev. B **71**, 214104 (2005).
[32] K. Momma and F. Izumi, J. Appl. Crystallogr. **44**, 1272 (2011).
[33] P. B. Allen and R. C. Dynes, Phys. Rev. B **12**, 905 (1975).
[34] G. Parthasarathy and W. B. Holzapfel, Phys. Rev. B **37**, 8499 (1988).
[35] S. Grimme, J. Comput. Chem. **27**, 1787 (2006).
[36] M. Dallavalle, N. Sändig, and F. Zerbetto, Langmuir **28**, 7393 (2012).